Purinergic Signalling (2020) 16:213–229
https://doi.org/10.1007/s11302-020-09696-0

ORIGINAL ARTICLE

Analysis of purine receptor expression and functionality in alveolar epithelial cells

Cynthia Olotu[1] · Martina Kiefmann[1] · Cornelia Ronneburg[1] · Felix Lehmensiek[1] · Annelie Cuvenhaus[1] · Volker Meidl[1] · Alwin E. Goetz[1] · Rainer Kiefmann[1]

Received: 14 January 2020 / Accepted: 6 March 2020 / Published online: 31 March 2020

Abstract

Despite its fundamental role in providing an extensive surface for gas exchange, the alveolar epithelium (AE) serves as an immunological barrier through, e.g., the release of proinflammatory cytokines and secretion of surfactant to prevent alveolar collapse. Thus, AE is important for sustaining lung homeostasis. Extracellular ATP secreted by alveolar epithelial cells (AECs) is involved in physiological and pathological conditions and acts mainly through the activation of purine receptors (P2Rs). When studying P2R-mediated processes, primary isolated type II AECs (piAECs) still represent the gold standard in in vitro research, although their preparation is time-consuming and requires the sacrifice of many animals. Hence, cultivated immortalized and tumor-derived AEC lines may constitute a valuable alternative. In this work, we examined P2R expression and functionality in piAECs, in immortalized and tumor-derived AEC lines with the purpose of gaining a better understanding of purinergic signaling in different cell systems and assisting researchers in the choice of a suitable cell line with a certain P2R in demand. We combined mRNA and protein analysis to evaluate the expression of P2R. For pharmacological testing, we conducted calcium ($[Ca^{2+}]$) measurements and siRNA receptor knockdown. Interestingly, the mRNA and protein levels of $P2Y_2$, $P2Y_6$, and $P2X_4$ were detected on all cell lines. Concerning functionality, P2XR could be narrowed to L2 and piAECs while P2YR were active in all cell lines.

Keywords Purinergic · Calcium · Alveolar epithelial cells · ATP · Lung

Introduction

The alveolar epithelium (AE), consisting of type I and type II AE cells (AECs), is faced with a vast number of challenges. With every breath taken, the AE is exposed to inhaled pathogens and particles that escape the nasopharyngeal and mucociliary clearance of the upper and lower respiratory tract and thus constitutes an important immunological barrier function. The AE has to withstand cyclic stretching and perpetual shear stress during respiration; it needs to protect itself from desiccation and alveolar edema through sensitive maintaining of alveolar surface fluid balance, upholds the surface tension to prevent alveolar collapse; and it essentially ensures gas exchange [1–3].

In the last years, growing evidence has shown that in addition to its function as the universal energy source, ATP is involved in the pathogenesis of lung diseases, promoting inflammation as a damage-associated molecular pattern [4], increasing the survival of tumor cells [5], and amplifying acute lung injury [6]. In resting cells, the intracellular concentration of ATP is within the millimolar range, whereas the extracellular concentration of this nucleotide is much lower, in the nanomolar range [7]. In AECs, a rise in ATP secretion is triggered, for example, by aggravated airflow, by cellular stretching, by changes in mucus hydration, and during lung disease and infection [8–13]. After secretion out of the cell, ATP acts as a paracrine messenger and is involved in the activation of purinergic receptors (P2Rs) [14–16]. P2Rs are

Martina Kiefmann and Cynthia Olotu contributed equally to this work.

Electronic supplementary material The online version of this article (https://doi.org/10.1007/s11302-020-09696-0) contains supplementary material, which is available to authorized users.

✉ Cynthia Olotu
c.olotu@uke.de

[1] Experimental Laboratory of the Department of Anesthesia, University Medical Center Hamburg-Eppendorf, Martinistrasse 52, 20247 Hamburg, Germany

divided into two major families of P2X and P2Y receptors (P2XRs and P2YRs). P2XRs, consisting of seven subgroups, form a cellular membrane-spanning pore and serve as an ionic channel upon activation, increasing the cell's permeability for cations and small ions. In contrast, P2YRs are seven-transmembrane-domain G protein-coupled receptors and consist of eight subgroups [10–12, 17–19]. P2YRs can be further divided into $P2Y_1$- and $P2Y_{12}$-like families. The latter includes $P2Y_{12}$, $P2Y_{13}$ and $P2Y_{14}$ receptors, which share considerable sequence homology and couple to G_i-proteins. Activation of the remaining P2YRs of the $P2Y_1$-like family, namely $P2Y_1$, $P2Y_2$, $P2Y_4$, $P2Y_6$, and $P2Y_{11}$, results in interaction with $G_{q/11}$ or G_s, activating PKC and IP_3 pathways and facilitating the release of calcium from the endoplasmic reticulum (ER). An increase in cytosolic calcium concentration ($[Ca^{2+}]_{cyt}$) is the common final path of many purinergic signaling cascades [17, 20, 21].

P2Rs are commonly found on virtually all AEC subtypes and cell lines; however, their expression profiles and even their functional activity are not yet completely characterized [22–26]. Nevertheless, knowledge of purinergic receptor expression is crucial when downstream ATP-mediated effects or purinergic signaling cascades are to be analyzed. Primarily isolated AECs are still considered the gold standard when performing in vitro research of pulmonary cellular signaling pathways. It remains a controversial issue whether immortalized cell lines can serve as an appropriate alternative in this context. Here, we examined P2Rs expression and functionality in AECs, comparing the commonly used human adenocarcinoma cell line A549 to primarily isolated rat type II AECs (piAECs) and to the immortalized rat alveolar cells lines L2, R3/1, and RLE, with a specific focus on ATP-induced $[Ca^{2+}]_{cyt}$ changes.

Materials and methods

Materials

Fluorophore Fura 2-AM (10 μM) was dissolved in 0.02% pluronic (both from PromoKine, Heidelberg, Germany). The agents ethylene glycol-bis (ß-aminoehtylether)-N,N′,N″ tetraacetic acid (EGTA 500 μM), ethylenediamintetraacetic acid (EDTA; 500 μM), ATP, UDP, UTP, α, β-methyleneATP (α,β-meATP), 2-methylthioATP (2-meSATP), and 2′(3′)-O-(4-benzoylbenzoyl)ATP (Bz-ATP) (all agonists, 100 μM) were purchased from Sigma-Aldrich (St. Louis, MO, USA). The antagonists A438079 hydrochloride (10 μM), 5-(3-Bromophenyl)-1,3-dihydro-2H-benzofuro(3,2-e]-1,4-diazepin-2-one (5-BDBD, 10 μM), and AR-C 118925XX (10 μM) were bought from Tocris Bioscience (Minneapolis, MN, USA). Solutions and agents were dissolved in Hank's balanced salt solution (HBSS) buffer (150 mM Na^+, 5 mM K^+, 1 mM Ca^{2+}, 1 mM Mg^{2+}, and 20 mM HEPES at pH 7.4). Antagonists were dissolved in dimethyl sulfoxide. To establish Ca^{2+}-free conditions, we used Ca^{2+}-free HBSS buffer containing 500 μM EGTA.

Cell culture

A549 cells (DSMZ, Braunschweig, Germany) were grown in F-12K medium (ATCC, Manassas, VA, USA) supplemented with 10% fetal bovine serum (FBS, Biochrom AG, Berlin, Germany), 10,000 U/ml penicillin and 10,000 μg/ml streptomycin (Biochrom) at 37 °C with 5% CO_2.

L2 rat alveolar epithelial cells (L2) and R3/1 rat alveolar epithelial cells were kindly provided by Thea Koch (University of Dresden, Dresden, Germany). The cells were grown in T75 flasks at 37 °C with 5% CO_2 in DMEM (Biochrom) supplemented with 10% FBS, 10,000 U/ml penicillin and 10,000 μg/ml streptomycin in an incubator.

Rat alveolar type II cells (RLE-6TN, LGC Standards GmbH, Wesel, Germany) were grown in Ham's F12 medium supplemented with 0.01 mg/ml bovine pituitary extract, 0.005 mg/ml insulin, 0.00125 mg/ml transferrin (all from Sigma-Aldrich), 2.5 ng/ml insulin-like growth factor I, 2.5 ng/ml epidermal growth factor (both from PeproTech Inc., Rocky Hill, NJ, USA), 10% FBS, 10,000 U/ml penicillin and 10,000 μg/ml streptomycin. All cells were cultured at 37 °C with 5% CO_2.

Primary type II AEC isolation and culture

Male Sprague Dawley rats (300 g) were purchased from Charles River (Sulzfeld, Germany). After review and approval by the local committee and the government of Hamburg, rats were treated humanely following the "principles of laboratory animal care." The isolation and culture of type II AECs from adult rats were performed according to procedures described previously [27, 28]. Using this method, isolated type II AECs can secret surfactant in vitro, which is one of the key phenotypic endpoints to characterize type II AECs [29, 30]. Briefly, after injection of 100 mg/kg body weight (BW) Ketanest (Pfizer, New York, USA) and 20 mg/kg BW Rompun (Bayer, Leverkusen, Germany), the lungs were surgically exposed under sterile conditions. The pulmonary artery was cannulated, and the lungs were then perfused with 10 ml F–12 K medium supplemented with 25 mM HEPES three times to remove the blood. After multiple lavages (5 × 10 ml) via the cannulated trachea with 5 mM EDTA and 5 mM EGTA in phosphate-buffered saline (PBS) solution (Sigma-Aldrich), the lungs were explanted. Upon instillation of 20 ml warm F-12K medium enriched with 50 mM HEPES and 4.5 units/ml elastase Grade II (Worthington, Lakewood, New Jersey, USA), the lungs were incubated at 37 °C for 30 min. After dissection of the large airways, the lungs were added to

20 ml F-12 K medium containing 25 mM HEPES, 20% FBS, and 100 μg/ml DNase (Type IV, Sigma-Aldrich), quickly minced and incubated at room temperature for 10 min. Then, the solution was mixed by end-over end-rotation for 4 min and filtered successively through cotton gauze (1, 2, and 4 ply, Fuhrmann, Munich, Germany) following filtration through a nylon mesh (100 and 40 μm, Corning, New York, USA). Upon centrifugation of the cell suspension at 150×*g* for 10 min and resuspension in 20 ml warm DMEM, the cells were applied to plates covered with rat IgG (Sigma-Aldrich) for 1 h at 37 °C. The non-adherent cells were removed, collected in sterile tubes, twice centrifuged at 150×*g* for 10 min and resuspended in 3 ml of culture medium (DMEM with 10% FBS, penicillin 10,000 U/ml, streptomycin 10,000 μg/ml and keratinocyte growth factor 10 ng/ml (Sigma-Aldrich)). After the determination of cell number and viability, the cells were plated on collagen-treated coverslips and incubated at 37 °C and 5% CO_2. To slow the dedifferentiation of AEC II to AEC I in vitro, the keratinocyte growth factor was added to the culture medium. This growth factor leads to the maintenance of type II AECs such as the expression of surfactant protein C and prevents the expression of aquaporin 5, an AEC type I specific marker, for up to 7 days in vitro [31]. To distinguish between piAECs types I and II, laminar bodies were labeled with the fluorophore LysoTrackerGreen (LTG) (Molecular Probes, Thermo Fischer Scientific, Waltham, MS, USA). As these organelles only occur in type II cells, LTG-positive cells were defined respectively. The type II purity of the isolated cell population was approximately 75%.

Ca^{2+}-imaging by fluorescence microscopy

The cells were placed on coverslips, loaded with Fura 2-AM in HBSS buffer, pH 7.3, and incubated for 30 min at 37 °C in the dark. Using epifluorescence microscopy with a dual excitation wavelength (Olympus, Hamburg, Germany), Ca^{2+} quantification was performed. The cells that underwent appropriate intervention and changes in fluorescence were measured using the mercury arc lamp illumination directed through 340-nm and 380-nm interference filters (Semrock, Rochester, NY, USA). The fluorophore exposure was controlled by a filter wheel (Sutter Lambda 10-C, Sutter Instrument Co., Novato, CA, USA). The fluorescence emission was measured at 510 nm using an objective lens (× 40, water immersion, numerical aperture 0.8, Zeiss, Göttingen, Germany) and a charge-coupled device camera (Coolsnap HQ2, Photometrics, Tucson, AZ, USA). The Ca^{2+}-concentrations were calculated from computer-generated 340/380 nm ratios based on a dissociation constant of 224 nmol/l and the appropriate calibration parameters [32].

Real-time quantitative RT-PCR

Total RNA was isolated using the RNeasy Kit (Qiagen, Hilden, Germany). For the cDNA synthesis, 2 μg of RNA were used in the Omniscript Reverse Transcription Kit (Qiagen) according to the manufacturer's instructions. RT-qPCR was performed with gene- and species-specific primers for the purinergic receptors $P2Y_1$, $P2Y_2$, $P2Y_4$ $P2Y_6$, $P2Y_{11}$, $P2Y_{12}$, $P2Y_{13}$, $P2Y_{14}$, $P2X_1$, $P2X_2$, $P2X_3$, $P2X_4$, $P2X_5$, and $P2X_7$ (Tables 1 and 2). The primers were chosen to span exon-exon junction to exclude contamination with genomic DNA. The cDNA template was amplified on a LigthCycler® 96 (Roche) according to the manufacturer's protocol. The normalization of the amplification products was performed using stable housekeeping genes of the respective cell line. We used ß-2-Microglobulin for L2, R3/1, and piAECs, beta-actin for RLE, and the ATP synthase subunit beta for A549 cells. The relative quantification of data was conducted using the Relative Expression Software Tool (REST, version 9).

Western blotting

Cells were lysed in RIPA-buffer supplemented with the protease inhibitor cocktail complete Mini EDTA free (Roche, Mannheim, Germany) for 30 min on ice. Cell lysates were centrifuged at 12,000×*g* for 20 min at 4 °C. Whole cell lysates (20 μg) were reduced in sample buffer (NuPage sample buffer, Life Technologies GmbH, Darmstadt, Germany) and reducing agent (NuPage sample reducing agent, Life Technologies GmbH) at 95 °C for 5 min. The samples were separated by a 4–12% Bis-Tris polyacrylamide gel (NuPage, Life Technologies GmbH) and transferred to nitrocellulose filters (Life Technologies GmbH) by electroblotting. After addition of blocking buffer (PBS plus 0.1% Tween containing 5% milk powder) followed by agitation for 1 h, specific P2R antibodies were applied overnight at 4 °C ($P2Y_2$, $P2Y_4$, $P2Y_6$, $P2Y_{12}$, $P2Y_{13}$, $P2X_3$, $P2X_4$, $P2X_5$, and $P2X_7$ from Alomone Labs, Jerusalem, Israel; $P2Y_1$ from Genway, San Diego, CA, USA; and $P2Y_{14}$ from Abcam, Cambridge, UK). Bound primary antibodies were visualized using horseradish peroxidase-conjugated secondary antibodies (1 h at room temperature with agitation) and enhanced chemiluminescent substrate (ECL) reagent (ECL Plus Western Blotting Detection Reagents, GE Healthcare, Freiburg, Germany) according to the manufacturer's protocol. For molecular weight standards, we used a MagicMark™ XP protein ladder (Life Technologies). The specificity of the antibodies was evaluated using specific antigens or positive controls.

Protein determination

Protein concentrations were determined by using a bicinchoninic acid (BCA protein assay kit, Thermo

Table 1 P2X-receptor oligo sequences used for RT-qPCR

$P2X_1$	Human	Forward	5′-CTG GCT GAG AAG GGT GGA GTG GTT GG-3′
		Reverse	5′-TGG CCC CAT GTC CTC AGC GTA TTT G-3′
	Rat	Forward	5′-GAA GTG TGA TCT GGA CTG GCA CGT-3′
		Reverse	5′-GCG TCA AGT CCG GAT CTC GAC TAA-3′
$P2X_2$	Human	Forward	5′-GCT GCT CAT CCT GCT CTA CTT CGT GTG G-3′
		Reverse	5′-GGG GTA GTG GAT GCT GTT CTT GAT GAG G-3′
	Rat	Forward	5′-GTG GTA CGT CTT CAT CGT GC-3′
		Reverse	5′-GAA CCC TCA TGC TCT CTG GG-3´
$P2X_3$	Human	Forward	5′-ATC AAC CGA GTA GTT CAG C-3′
		Reverse	5′-GAT GCA CTG GTC CCA GG-3′
	Rat	Forward	5′-TGG CGT TCT GGG TAT TAA GAT CGG-3′
		Reverse	5′-CAG TGG CCT GGT CAC TGG CGA-3′
$P2X_4$	Human	Forward	5′-GAG ATT CCA GAT GCG ACC-3′
		Reverse	5′-GAC TTG AGG TAA GTA GTG G-3′
	Rat	Forward	5′-GAG GCA TCA TGG GTA TCC AGA TCA AG-3′
		Reverse	5′-GAG CGG GGT GGA AAT GTA ACT TTA G-3′
$P2X_5$	Human	Forward	5′-AGC ACG TGA ATT GCC TCT GCT TAC-3′
		Reverse	5′-ATC AGA CGT GGA GGT CAC TTT GCT C-3′
	Rat	Forward	5′-GCC GAA AGC TTC ACC ATT TCC ATA A-3′
		Reverse	5′-CCT ACG GCA TCC GCT TTG ATG TGA TA**G**-3′
$P2X_7$	Human	Forward	5′-CCC CGG CCA CAA CTA CAC CAC GAG AAA C-3′
		Reverse	5′-CCG AAG TAG GAG AGGGTTGAG CCG ATG-3′
	Rat	Forward	5′-GTG CCA TTC TGA CCA GGG TTG TAT AAA-3′
		Reverse	5′-GCC ACC TCT GTA AAG TTC TCT CCG ATT-3′
ATP5B	Human	Forward	5′-ACT ACG CCA TGT TGG GGT TT-3′
		Reverse	5′-CGC ATA GTC CCT GAC AGG AT-3′
B2m-1	Rat	Forward	5′-TGT CTC AGT TCC ACC CAC CT-3′
		Reverse	5′-ATT ACA TGT CTC GGT CCC AGG-3′

Scientific, Rockford, IL, USA) according to the manufacturer's instructions.

SiRNA knockdown of P2Rs

The cells were transfected with 10 nM siRNA for $P2Y_2$-, $P2Y_6$-, $P2Y_4$-, $P2X_4$-, $P2X_5$-R (Qiagen), or scrambled siRNA (Qiagen), respectively, using the transfection reagent Lipofectamine RNAiMAX (Life Technologies GmbH) according to the manufacturer's protocol. The siRNA (20 μM) was diluted in serum-free 500 μl Opti-MEM (Life Technologies) to obtain a 10 nM siRNA solution in the indicated coverslips or center dishes. The transfection reagent (1:10) was added to each coverslip/center dish. Upon 15 min of incubation, 125,000 cells diluted in 2.0 ml complete growth medium (without antibodies) were added to each coverslip/center dish. Following 48 h of incubation, the transfected cells underwent RT-qPCR analysis to confirm successful knockdown or Ca^{2+} imaging to evaluate the functional consequences of receptor knockdown.

Statistical analysis

The results of the mRNA expression analysis were presented as the mean ± SD of the values obtained from the indicated number of experiments. The results for the calcium imaging were presented as the median ± 75% and 25% quartile of the values obtained from the indicated number of experiments. The analysis was performed using paired or unpaired *t* tests with equal variances for dependent and independent variables, respectively. The results were adjusted according to the method of Bonferroni. The statistical calculations were performed using the software of the R project for statistical computing ("R"). Statistical significance was accepted at $p < 0.001$.

Results

MRNA detection of purinergic receptors

First, the AECs were screened for the presence of P2R mRNA. Concerning P2XR, a heterologous appearance

Table 2 P2Y-receptor oligo sequences used for RT-qPCR

$P2Y_1$	Human	Forward	5′-CCC TGG GCC GGC CTC AAA AAG AAG AAT G-3′
		Reverse	5′-CAA GCC GGG CCC TCA AGT TCA TCG TTT TC-3′
	Rat	Forward	5′-TCA GAA GGA GAC TGT CCC GA-3′
		Reverse	5′-CAG GGA CTT CTT GTG ACC ATG T-3′
$P2Y_2$	Human	Forward	5′-GCA GTG GCG AGA GGA GC-3′
		Reverse	5′-GAA CTC TGC GGG AAA CAG GA-3′
	Rat	Forward	5′-TAA AGA GGA ACG AAC ACC GGG-3′
		Reverse	5′-CCA GCC TCC AGC ATT TTT CA-3′
$P2Y_4$	Human	Forward	5′-CCA CCT GGC ATT GTC AGA CAC C-3′
		Reverse	5′-GAG TGA CCA GGC AGG GCA CGC-3′
	Rat	Forward	5′-CTG GAC TAA GGA AGC TAG GGG G-3′
		Reverse	5′-GGC TGG GAC CTA GTG ATG TG-3′
$P2Y_6$	Human	Forward	5′-GCT AAC TCT TGG CCT CCC TG-3′
		Reverse	5′-GTA GAC ACA GGT GGT GGG TG-3′
	Rat	Forward	5′-TCT TGC ATG AGA CAG ATT CTC CA-3′
		Reverse	5′-GCA GCA GTC GCT TGA AAT CC-3′
$P2Y_{11}$	Human	Forward	5′-GGC ACA ATG AGG AAG GAA ACG-3′
		Reverse	5′-CAG GAC TTG GCA CCC GAG AC-3′
$P2Y_{12}$	Human	Forward	5′-ATC TCT GAT TGT GAA GCC CTC T-3′
		Reverse	5′-TGG TGC ACA GAC TGG TGT TA-3′
	Rat	Forward	5′-TGC AAT GCC GAG AAC ACT CT-3′
		Reverse	5′-CCC CAC CTT CCT GTC CTT TC-3′
$P2Y_{13}$	Human	Forward	5′-CCT CCC AAA GGT GAC ACT GG-3′
		Reverse	5′-ACA AAC ACC CAC AGA GCC AA-3′
	Rat	Forward	5′-GTT CAT CCA CAT CCC CAG CA-3′
		Reverse	5′-CCC AGG GGA CTC TTT AGG GA-3′
$P2Y_{14}$	Human	Forward	5′-TCA TTG CGG GAA TCC TAC TC-3′
		Reverse	5′-CCC AAA GAA CAC AAT GCT GAC-3′
	Rat	Forward	5′-GTT GCC AGG ATC CCC TAC AC-3′
		Reverse	5′-ACT TTT CTG CGT GCT GTA GA-3′
ATP5B	Human	Forward	5′-ACT ACG CCA TGT TGG GGT T-3′
		Reverse	5′-CGC ATA GTC CCT GAC AGG AT-3′
B2m-1	Rat	Forward	5′-TGT CTC AGT TCC ACC CAC CT-3′
		Reverse	5′-ATT ACA TGT CTC GGT CCC AGG-3′

between the different cell lines was observed. For each P2R family member and cell type, the mRNA level of a particular subtype that was detected in all AECs was arbitrarily set as 1, and the expression of other P2Rs was displayed in relation to this value to facilitate comparisons (Fig. 1). $P2X_4R$ was chosen for the P2XRs family, and $P2Y_2R$ was chosen for the P2YR family, as considerable numbers of transcripts of both P2Rs were detected in all the AECs examined. Regarding P2XRs, $P2X_1R$ (in piAECs), $P2X_2R$ (in RLE), $P2X_3R$ (in L2, R3/1 and RLE), $P2X_5R$ mRNA (in L2 and A549), and $P2X_7R$ (in L2, RLE, and piAECs) were observed. Regarding P2YRs, $P2Y_2R$ and $P2Y_6R$ mRNA was detected in all AECs; $P2Y_4R$ mRNA was detected in the rat-derived cell lines L2, R3/1, RLE, and in piAECs, while $P2Y_1$ mRNA was detected in piAECs and A549 cells. In addition, $P2Y_{12}$-, $P2Y_{13}$-, and $P2Y_{14}$–mRNA was only found in piAECs.

Protein expression of purinergic receptors

Western blot analysis revealed that $P2X_4R$ and $P2Y_2R$ were the only P2Rs expressed in the AECs (Table 3 and Fig. 1 supplement) examined in this study. All other P2Rs displayed a heterologous distribution pattern. Concerning P2XRs, $P2X_5$ protein was found in L2 and A549, and $P2X_7R$ protein was found in piAECs and RLE (Table 3A and Fig. 1 supplement). Regarding the P2YR family, $P2Y_4R$ protein (in L2, R3/1, RLE, and A549) and $P2Y_6R$ protein (in L2, R3/1, piAECs, and A549) were detected (Table 3B and Fig. 1 supplement). We tested $P2Y_4R$ protein expression in A549 cells despite the lack of a positive mRNA transcript for this receptor as we were unable to distinguish between mRNA or genomic DNA in our RT-qPCR due to the absence of introns in the human $P2Y_4R$ gene [33].

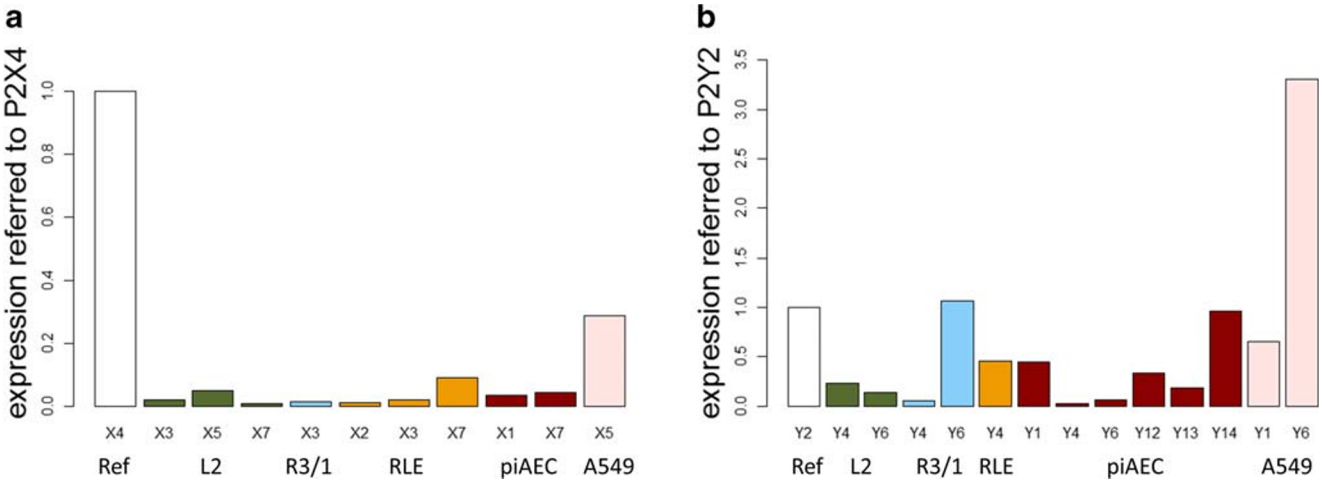

Fig. 1 mRNA expression of the P2 receptor genes using real-time quantitative RT-qPCR. The expression level of the receptors was normalized to their respective housekeeping genes. **a** The expression level of $P2X_4R$ was arbitrarily expressed as 1. The gene expression levels of the other P2XRs were expressed as relative values to that of $P2X_4R$. **b** The expression level of $P2Y_2R$ was arbitrarily expressed as 1. The gene expression levels of the other P2YRs were expressed as their relative values to that of $P2Y_2R$; $n = 3$ for each receptor and each AEC

Examination of P2R functionality after ATP stimulation

To examine P2R functionality in AECs, we focused on determining the cytosolic calcium levels. An increase in cytosolic calcium concentration $[Ca^{2+}]_{cyt}$ is one of the most immediate consequences of purinergic activation. To distinguish between type I and II piAECs, laminar bodies were labeled with the fluorophore LTG (Fig. 2). Because these organelles only occur in type II cells, LTG-positive cells were defined as type II AECs. piAECs $[Ca^{2+}]_{cyt}$ determinations were performed only in LTG-positive cells by merging LTG- and Fura-2-stained cells (Fig. 2).

In Fig. 3, the characteristic traces of real-time $[Ca^{2+}]_{cyt}$ courses under baseline condition and upon ATP stimulation for each AEC are shown.

Table 3 Expression of P2Rs in the respective cell lines detected by western blotting

A								
	$P2X_1$	$P2X_2$	$P2X_3$	$P2X_4$	$P2X_5$	$P2X_7$		
L2				X	X			
R3/1				X				
RLE				X		X		
piAECs				X		X		
A549				X	X			
B								
	$P2Y_1$	$P2Y_2$	$P2Y_4$	$P2Y_6$	$P2Y_{11}$	$P2Y_{12}$	$P2Y_{13}$	$P2Y_{14}$
L2		X	X	X				
R3/1		X	X	X				
RLE		X	X					
piAECs		X		X				
A549		X	X	X				

The baseline $[Ca^{2+}]_{cyt}$ ranged from 29 to 118 nM (L2: 46.4 nM, R3/1: 29.4 nM, RLE: 117.5 nM, piAEC: 91.9 nM, and A549: 88.6 nM; median values of each AEC) (Fig. 4A) and remained on this level if no further action was taken (the observation period was 150 min, data not shown). The cells were then stimulated with 100 μM ATP, an endogenous agonist of almost all P2Rs except $P2Y_{14}$, which is stimulated by nucleotide sugars and UDP [34, 35]. Exposure to ATP led to an immediate increase in $[Ca^{2+}]_{cyt}$ followed by a slow decrease (Fig. 3) (L2: 107.7 nM, R3/1: 98.9 nM, RLE: 184.4 nM, piAECs: 191.44 nM, and A549: 182.5 nM; median values of each AEC) (Fig. 4B).

To localize the source of the calcium increase, namely, extracellular, intracellular and/or both, calcium imaging was conducted in a calcium-depleted environment. The ionotropic P2XRs form a membrane-spanning ion channel upon activation by ATP, allowing large extracellular cations to permeate the cellular membrane [8]. Thus, applying a calcium-free environment prevents a P2XR-mediated Ca^{2+}-response (Fig. 4C). Exclusively in L2 and piAECs calcium-free conditions led to a significant decrease in the ATP-induced calcium response compared to that seen in a calcium-containing environment (L2: 9.8 nM, R3/1: 56.3 nM, RLE: 131.8 nM, piAECs: 45.2 nM and A549: 242.6 nM; median values of each AEC) (Fig. 4C and D). This result indicates a functional role for P2XRs in contributing to the ATP-induced $[Ca^{2+}]_{cyt}$ increase in L2 and piAECs but not in R3/1, RLE or A549 cells.

To evaluate the functionality of distinct P2R, we exposed piAEC and AEC lines to physiologically endogenous as well as synthetic P2R agonists (Figs. 5 and 6). UTP is considered a predominant agonist of $P2Y_2R$ and $P2Y_4R$, while UDP (100 μM) is a strong physiological agonist of $P2Y_6$ and $P2Y_{14}$ [9]. The UTP-induced response in the L2 cells was

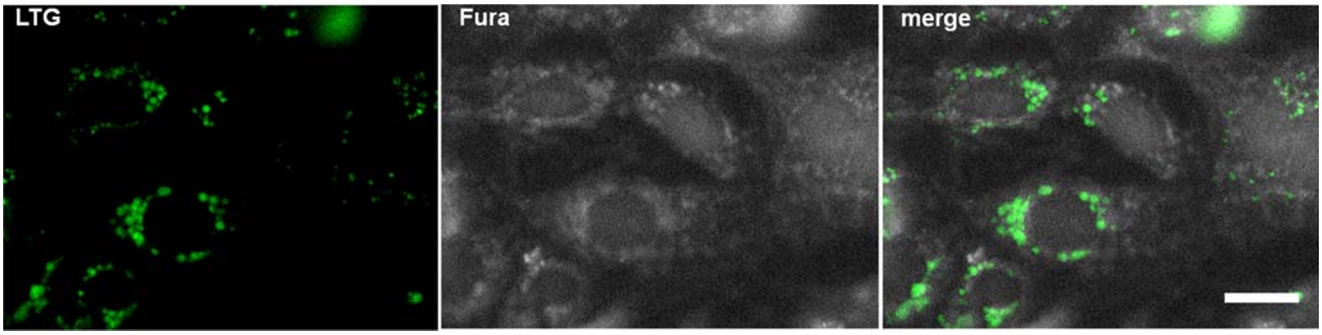

Fig. 2 Image of LTG-positive type II piAECs by immunofluorescence microscopy. Left: LTG staining; middle: Fura 2-AM staining; right: merged image of Fura 2-AM and LTG stained cells. White scale bar (right picture) is 10 μm

not as high as that upon ATP stimulation (16.45 nM), but in the R3/1, RLE, and A549 cells, UTP administration even exceeded stimulation with ATP (218.5 nM, 235.3 nM, and 1415.2 nM, respectively) (Fig. 5). As piAECs lacked $P2Y_4$ expression (Table 3B), UTP stimulation was unnecessary in these cells. The pyrimidine-based nucleotide UDP evokes an increase in $[Ca^{2+}]_{cyt}$ in the L2, R3/1 and piAECs (79.1 nM, 195.4 nM, and 38.4 nM, respectively). We did not test the endogenous agonist ADP because we could not detect P2Rs ($P2Y_1$, $P2Y_{12,}$ and $P2Y_{13}$), which are activated by this nucleotide, neither on piAECs nor on AECs. The synthetic P2R agonist α,β-meATP (100 μM) evoked only a slight calcium response in all respective AECs (Fig. 6). An agonist of $P2X_4$ and $P2X_{5,}$ 2-meSATP (100 μM), led to a significant calcium increase in the L2 (81.1 nM), R3/1 (83.8 nM), and A549 (16.9 nM) cells but not in the RLE or piAECs. Upon stimulation with BzATP, a strong agonist of $P2X_4$ and $P2X_7$, R3/1 (128.0 nM), RLE (871.1 nM), and piAECs (45.7 nM) displayed a significant increase in $[Ca^{2+}]_{cyt}$ (Fig. 6).

SiRNA knockdown of P2Rs

Taken together, data obtained from mRNA and protein determination as well as from functional testing indicated that $P2Y_2R$ (L2, R3/1, RLE, piAECs and A549), $P2Y_6R$ (L2, R3/1, and piAECs), $P2Y_4R$ (R3/1 and A549), $P2X_4R$ (L2), and $P2X_5R$ (L2) were the most likely candidates mediating the increase in $[Ca^{2+}]_{cyt}$ upon ATP stimulation in the AECs examined. To elucidate the proportion of a respective receptors' effect on the ATP-induced increase in $[Ca^{2+}]_{cyt}$, the cells were transfected with the respective siRNA. However, no P2R knockdowns could be achieved in piAECs, as these cells were unable to keep a type II state for the duration of the siRNA transfection process and instead dedifferentiated back to the type I phenotype. Therefore we performed pharmacological inhibition of respective receptors in piAECs in an additional set up. Figure 7A depicts the efficiency of the siRNA knockdowns for the respective AECs. Compared with scrambled siRNA, the functional active siRNA led to a distinct knockdown of all respective receptors in the AECs investigated (Fig. 7A). Functionally, $P2Y_2R$ knockdown inhibited the ATP-induced calcium response by 84.2%, 80.7%, 69.7%, and 100% in L2, R3/1, RLE, and A549 cells, respectively (Fig. 7B). The $P2Y_6$ R knockdown led to a 32.6% and 5.7% reduction in the ATP-induced calcium response in L2 and R3/1 cells, respectively. As our previous results indicate that $P2Y_4R$ is active in R3/1, we performed a knockdown of this receptor in R3/1 cells. As shown in Fig. 7B the calcium response was reduced by 93.4% upon stimulation with ATP. A $P2X_4R$ knockdown was performed in L2 as the ATP-induced calcium response in these cells depended partially on extracellular calcium. In L2 cells the $P2X_4$ R siRNA knockdown diminished the ATP-induced increase in $[Ca^{2+}]_{cyt}$ by 85.8%. Interestingly, knockdown of the functional active $P2X_5R$ in L2 cells resulted in an increase in $[Ca^{2+}]_{cyt}$ upon ATP (Fig. 7B).

Pharmacological inhibition of P2Rs

Due to the above-mentioned reasons, P2Rs were inhibited pharmacologically in piAECs. Three receptors, $P2Y_2R$, $P2X_4R$, and $P2X_7R$ were tested as candidates inducing the rise in $[Ca^{2+}]_{cyt}$ upon ATP stimulation. The application of each antagonist led to a significant decrease in ATP-triggered elevation in $[Ca^{2+}]_{cyt}$. $P2Y_2R$-antagonist AR-C118925XX reduced the $[Ca^{2+}]_{cyt}$ increase by 83.2%, $P2X_4R$-antagonist 5-BDBD led to a reduction by 74.6%, and $P2X_7R$-antagonist A438079 by 81.0% compared with that of the ATP-induced $[Ca^{2+}]_{cyt}$ response in native piAECs (Fig. 8).

Discussion

In the lung, ATP acts as an important signaling molecule to ensure functions such as mucociliary clearance, control of local blood flow, and surfactant secretion in the alveolus through type II AECs [36, 37]. The release of ATP in the alveolus is triggered by multiple stimuli, such as mechanical stress caused by stretch and surface tension forces [38], pro-inflammatory thrombin stimulation [39], and hypotonic shock

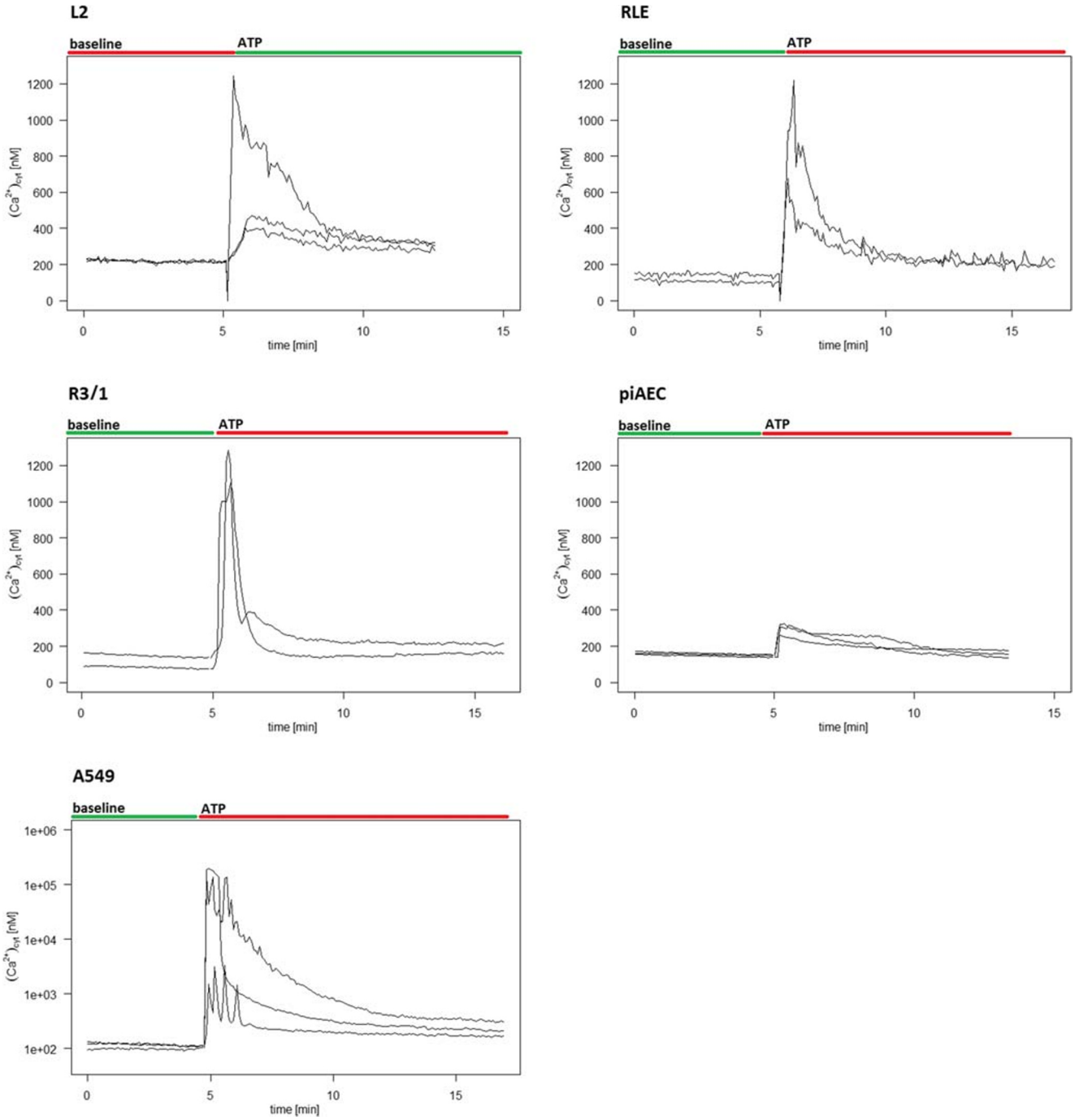

Fig. 3 Tracing of $[Ca^{2+}]_{cyt}$ under the baseline condition followed by ATP (100 μM) stimulation in L1, R3/1, RLE, piAECs, and A549 (as indicated). Representative result for at least 10 experiments of each AECs

[40]. Secreted ATP acts in an auto- and/or paracrine manner through the activation of P2Rs.

P2Rs mediate a wide range of cellular functions. They are expressed ubiquitously in eukaryotes, and the effects mediated through them are often specific to the respective tissue [11, 12, 19, 41]. Due to the diversity of P2R-mediated effects, these receptors are promising targets for therapeutic approaches against a diversity of diseases, e.g., $P2Y_{12}R$ antagonists have been widely established as antiplatelet drugs [42, 43]. Antagonists of $P2X_7$ are under evaluation for rheumatoid arthritis treatment [44]. P2R research is an evolving field of growing interest and demand. Cell culture experiments remain a favorable tool to examine purinergic signaling in vitro and to further analyze the molecular mechanisms and downstream cellular effects. Although primary isolated cells are still the gold standard of in vitro studies, the isolation of primary rat or mouse AECs is complex, time-consuming, and requires the sacrifice of many animals. Hence, many cultivated AEC lines,

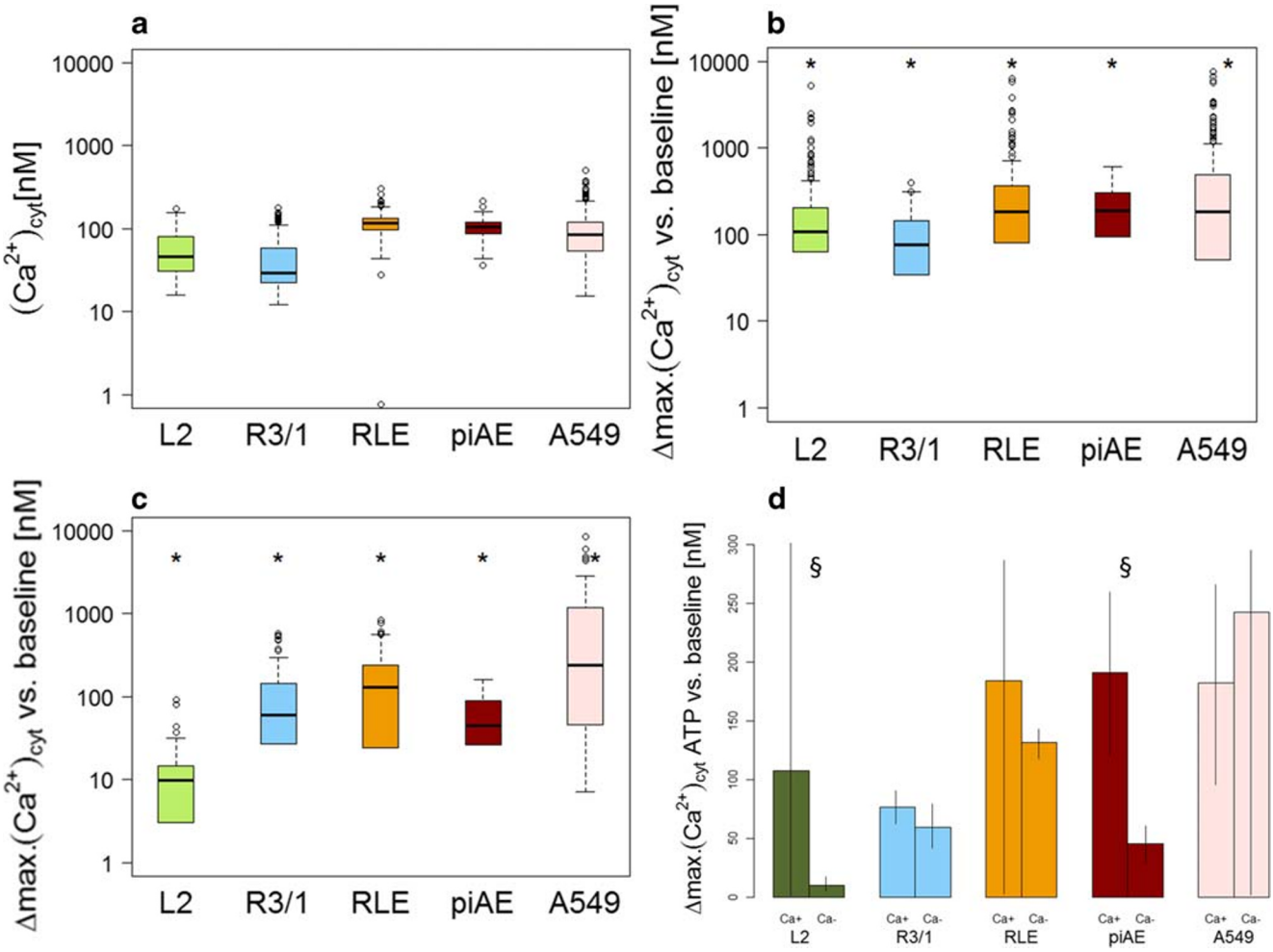

Fig. 4 $[Ca^{2+}]_{cyt}$ in L2, R3/1, RLE, piAECs, and A549. **a** $[Ca^{2+}]_{cyt}$ under baseline conditions, **b** upon 100 μM ATP treatment in calcium-containing medium, **c** upon 100 μM ATP treatment in calcium-free medium, and **d** a comparison of $[Ca^{2+}]_{cyt}$ upon ATP (100 μM) stimulation in calcium-containing or calcium-free medium. Differences between the maximum and baseline $[Ca^{2+}]_{cyt}$ (Δ: delta) are displayed as box plots, with median values ± 75% and 25% quartiles, $n = 6–31$, * $p < 0.001$ vs. baseline conditions, § $p < 0.001$ vs. calcium-containing conditions

tumor-derived or immortalized, have been established. However, the characterization of P2R expression, as well as their functional assessment in the available cell lines, often remains incomplete. Here, we attempted a systematic characterization of the functional P2R expression profile on primary isolated type II AECs and selected AEC lines with particular regard to ATP-induced elevations in $[Ca^{2+}]_{cyt}$. We chose an escalating process by first analyzing the presence and amount of P2R mRNA in the respective AECs followed by the determination of specific P2R protein expression. To reveal P2R reliability, we stimulated primary isolated and immortalized AECs with the physiologically endogenous P2R agonist ATP. To evaluate the functionality of distinct P2Rs, UDP and UTP, as well as specific synthetic agonists were tested. Finally, P2R siRNA knockdown allowed the determination of the share of each functional P2R in the respective AEC lines regarding the ATP-induced calcium response. To the knowledge of the authors, this is the first study investigating the expression and functional P2R profile of rat piAECs in comparison with those of the human A549 adenocarcinoma cells and other immortalized AEC lines.

Our results show that concerning P2R mRNA, P2XRs present much greater heterogeneity than P2YRs. However, the mRNAs of almost all P2R subtypes ($P2XR_{1, 2, 3, 4, 5, and 7}$ and $P2YR_{1, 2, 4, 6, 12, 13, and 14}$) except $P2YR_{11}$ were distributed among the AECs examined in this work. As Kügelgen and Hoffmann [45] reported, $P2Y_{11}R$ cannot be found in the rat genome. However, we were unable to detect $P2Y_{11}R$ in human A549 cells, which stands in contrast to previously published data [5, 46]. The reason for this discrepancies may underlie the used primer sets for detection of the $P2Y_{11}R$ mRNA, since Dreisig and Kornum [47] reported that the $P2Y_{11}R$ gene and the PPAN gene are located on the same chromosome in humans. These two genes have been found to build a fusion transcript that shares much of its sequence with the $P2Y_{11}R$ mRNA, so primer sets intended to detect $P2Y_{11}R$ mRNA transcripts must be especially carefully designed unless the fusion transcript might not be amplified.

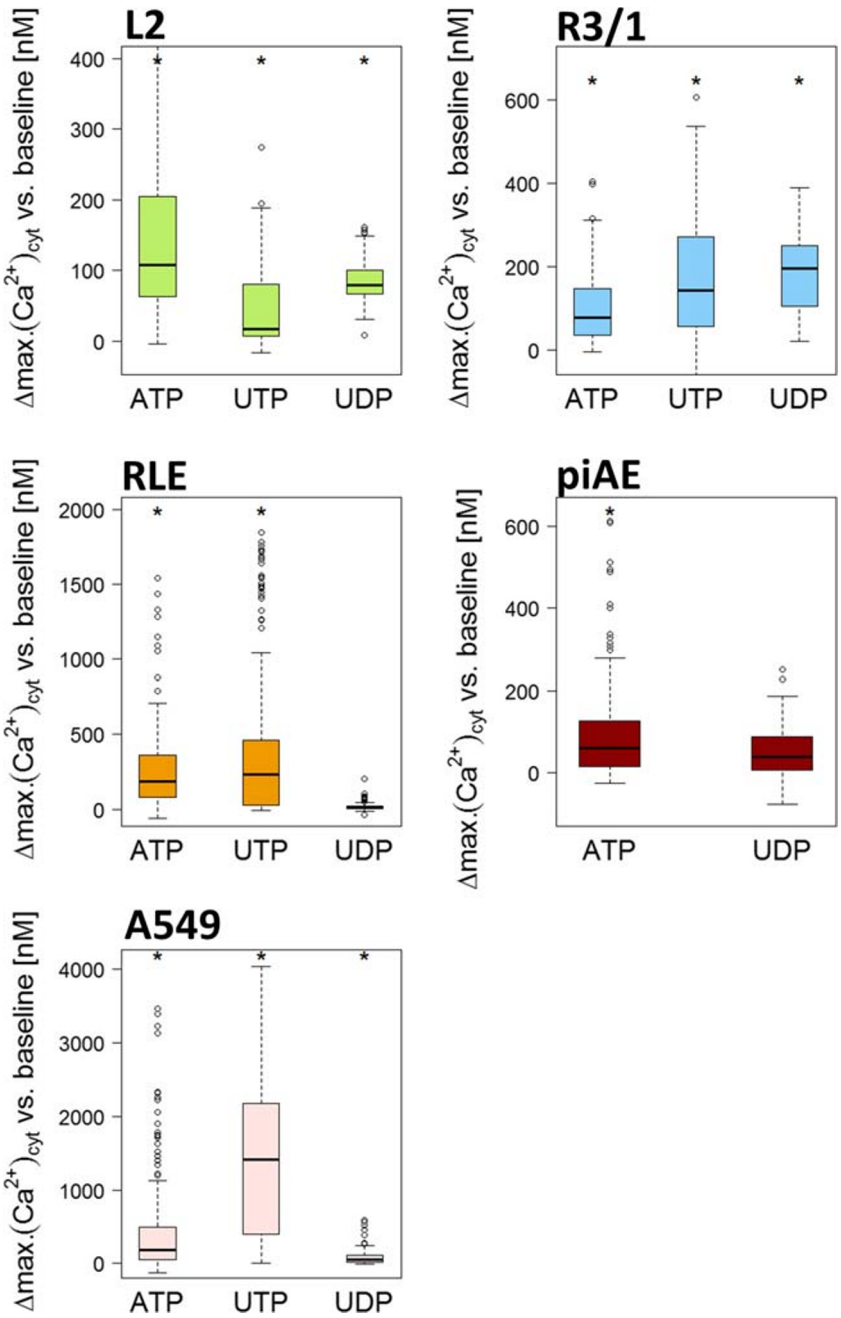

Fig. 5 $[Ca^{2+}]_{cyt}$ in the L2, R3/1, RLE, piAECs, and A549 cells upon stimulation with ATP, UTP, and UDP (all 100 μM). Displayed are differences between the maximum and baseline $[Ca^{2+}]_{cyt.}$ (Δ: delta) as box plots, with median values ± 75% and 25% quartiles, $n = 3–31$, * $p < 0.001$ vs. baseline conditions

Commonly, the presence of mRNA does not necessarily result in protein expression. $P2X_4R$ is implicated in the secretion of surfactant from lamellar bodies upon ATP stimulation [25, 48]. Lamellar bodies are organelles of type II AECs, and secretion of surfactant is one of the main challenges of these cells. Therefore, it is not surprising that all investigated AECs expressed $P2X_4R$ protein. The other P2XRs were expressed in different patterns among the cell lines investigated in this study. In L2, RLE, piAECs, and A549 cells, but not R3/1 cells, P2XR protein were found, wherein L2 and A549 cells expressed $P2X_5R$ and RLE cells and piAECs expressed $P2X_7R$. $P2X_7R$ is suggested to be involved in the inflammatory response mediated by the inflammasome pathway through the release of TNF-α or IL-1ß [49, 50]. The strong expression of $P2X_7R$ in piAECs, in contrast to its weak expression in RLE cells and the absence of $P2X_7R$ in the other AEC lines investigated, may reflect adaption to the environmental conditions of the rats, which were held under specific pathogen-free conditions. However, it cannot be ruled out that the expression of $P2X_7R$ on piAECs is caused by the remaining type I piAECs or alveolar macrophages since the purity of the isolated type II piAECs was approximately 75%. However, BzATP triggered a calcium response only in the LTG-stained cells, i.e., type II AECs and piAECs. Therefore,

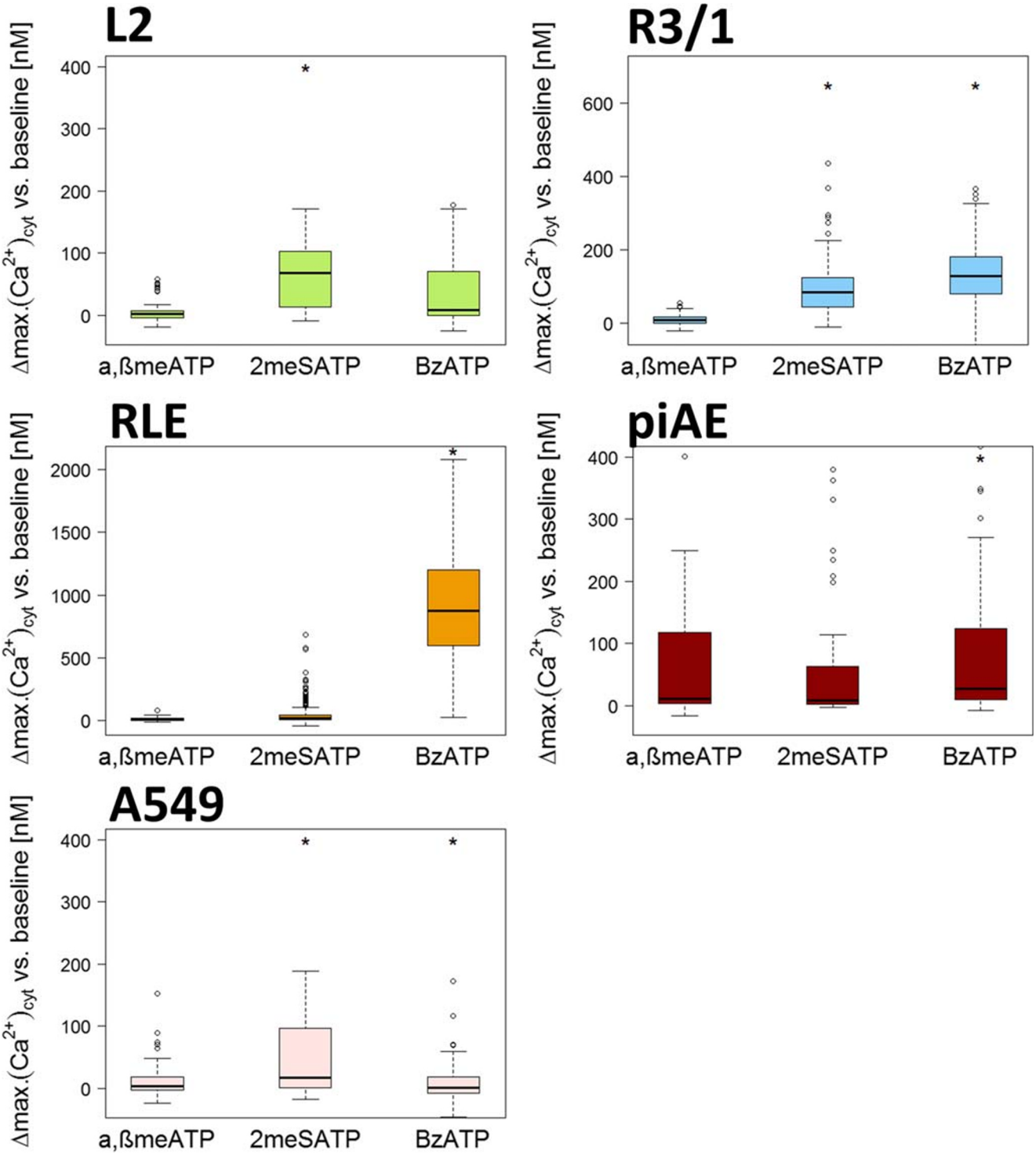

Fig. 6 $[Ca^{2+}]_{cyt}$ in L2, R3/1, RLE, piAECs, and A549 upon stimulation with β-meATP, 2-meATP, and BzATP (100 μM). Displayed are differences between the maximum and baseline $[Ca^{2+}]_{cyt.}$ (Δ: delta) as box plots, with median values ± 75% and 25% quartiles, $n = 3–20$, * $p < 0.001$ vs. baseline conditions

it can be concluded that $P2X_7R$ is expressed on type II piAECs. This is in contrast to the work by Chen et al. [51], who stated that $P2X_7R$ was a potential marker for the identification of type I piAECs. The expression of $P2X_5R$ in A549 cells can be explained by its involvement in tumor-associated processes. Consistent with this, it has been reported that other cell lines derived from adenocarcinomas, such as PC-3 and MDA-MB-468 cells, also express $P2X_5R$ [52, 53]. $P2X_5R$ mRNA transcripts have been detected in cells of the immune system [54]; however, the expression pattern and function of

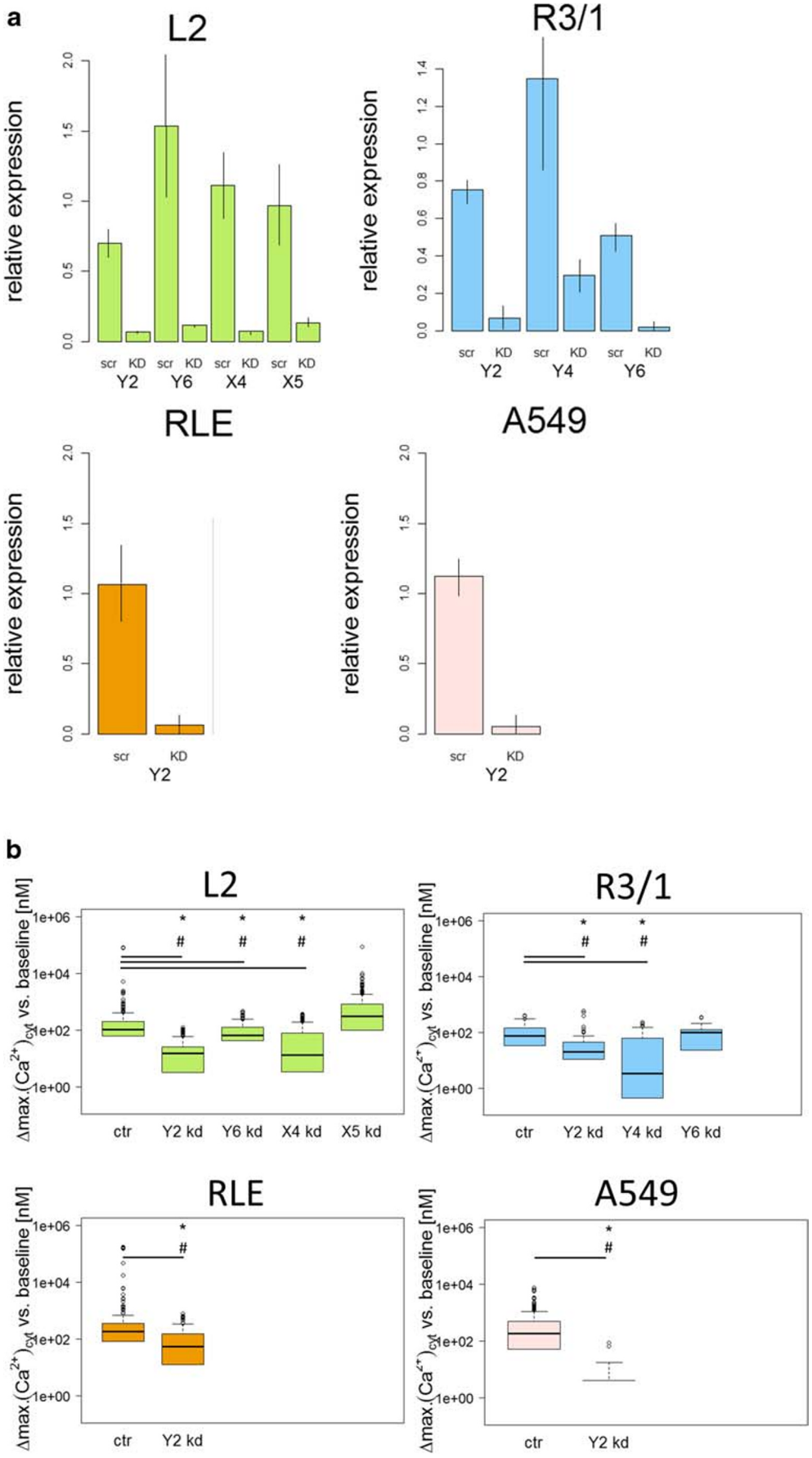
a
L2
R3/1
RLE
A549
relative expression
scr
KD
Y2
Y6
X4
X5
Y4
b
L2
R3/1
RLE
A549
Δmax.(Ca2+)cyt vs. baseline [nM]
ctr
Y2 kd
Y6 kd
X4 kd
X5 kd
Y4 kd

◀ **Fig. 7** siRNA knockdown experiments of selective P2 receptors in L2, R3/1, RLE, and A549 cells. **a** Relative expression of the P2 receptor genes after siRNA knockdown using real-time quantitative RT-PCR (scr: scramble siRNA; KD: respective siRNA as indicated), $n = 3–4$ for each receptor and each AEC line investigated, mean ± SD. **b** $[Ca^{2+}]_{cyt}$ following stimulation with ATP (100 μM) after siRNA knockdown as indicated. Displayed are differences between maximum and baseline $[Ca^{2+}]_{cyt.}$ (Δ: delta) as box plots, with median values ± 75% and 25% quartiles, $n = 10–31$, * $p < 0.001$ vs. baseline conditions, # $p < 0.001$ vs ctr

$P2X_5R$ in humans is still unclear. Among the eight subgroups of P2YRs, only three different types were expressed in the investigated AECs. $P2Y_2R$ protein was detected in all AECs; however, $P2Y_4R$ protein was found on L2, R3/1, RLE, and A549 cells, and $P2Y_6R$ protein was detected on L2 cells, R3/1 cells, piAECs, and A549 cells. Since $P2Y_2R$, like $P2X_4R$, plays a role in surfactant secretion, it is not surprising that all AECs express this receptor [55].

Upon stimulation with ATP, all AECs displayed an increase in $[Ca^{2+}]_{cyt}$, although in distinct quantities. In a calcium-depleted environment, however, this increase was reduced in L2 cells, R3/1 cells, and piAECs but remained almost unaltered in RLE and A549 cells. In these two AEC lines, a prevailing functional role for P2YRs initiating calcium release from the endoplasmic reticulum upon ATP activation seems likely. The L2, R3/1 and piAECs results indicate a functional coexistence of P2YRs with P2XRs. This has already been described in other tissues, such as cerebellar granule cells, smooth muscle, and sensory neurons [56–58].

Exposure of AECs to additional endogenous and synthetic P2R agonists allowed us to further evaluate the potentially functional P2 as well as to identify receptors responsible for the ATP-induced $[Ca^{2+}]_{cyt}$ changes. The endogenous nucleotides comprise UTP and UDP, which only activate P2YRs and not P2XRs. These cationic channels are stimulated solely through the endogenous agonist ATP [10, 16, 18]. Synthetic agonists were selected based on the results of the P2R western blot analysis for each respective AEC line. Taken together, the data on the stimulation with specific agonists confirmed our findings on P2R expression in AECs and prompted us to perform siRNA knockdown experiments to further characterize the role of the respective P2Rs responsible for the ATP-induced $[Ca^{2+}]_{cyt}$ increase in AECs. Concerning L2 cells, P2XRs seemed to play a predominant role, as the calcium response to ATP was almost entirely dependent on extracellular calcium. However, there seemed to be a different population of cells solely expressing functional $P2Y_2R$ or $P2Y_6R$, explaining the reduction in, but not the extinction of the ATP-induced calcium response after their specific knockdown. As the response to ATP remained an all-or-nothing reaction for every single cell, the coexistence of a $P2X_4R$-, a $P2Y_2R$- and a small $P2Y_6R$-expressing subpopulation was assumed, rather than a general L2 population expressing all three P2 receptor types. Similar findings have been described by Volonte et al., who consider the possibility of cellular subpopulations expressing different P2Rs as well as having different P2R profiles on the apical and basolateral membranes of the same cell [59]. The $P2X_5R$ seems to play no role in the ATP-triggered rise of $[Ca^{2+}]_{cyt}$ since the knockdown resulted in no reduction but in a slight increase of $[Ca^{2+}]_{cyt}$ upon ATP stimulation. In R3/1 cells the knockdown of $P2Y_2R$, and $P2Y_4R$ resulted in a strongly diminished $[Ca^{2+}]_{cyt}$ increase whereas the downregulation of the $P2Y_6R$ expression developed only a little impact on the calcium release upon ATP stimulation. In RLE-, as well as in R3/1 cells P2XRs expression plays a minor role, considering the results obtained under calcium-free conditions where the ATP induced increase was not significantly

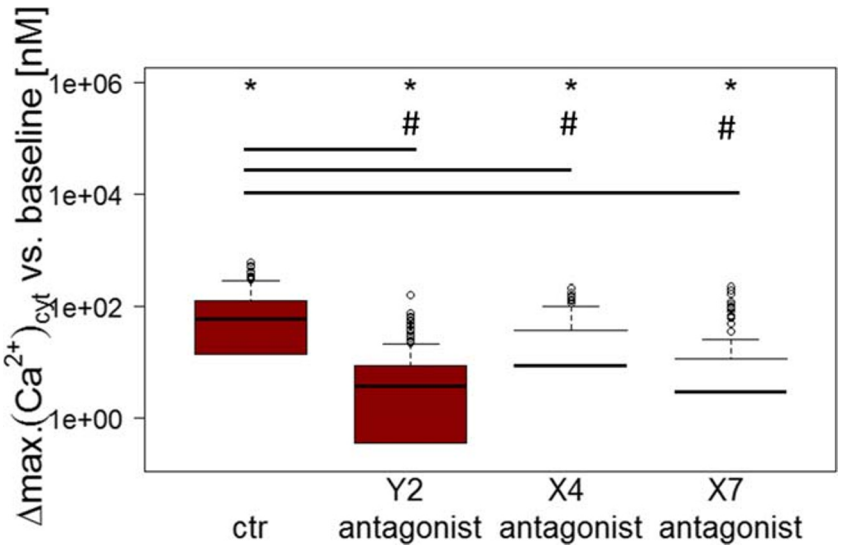

Fig. 8 Pharmacological inhibition of selective P2 receptors in piAECs. $[Ca^{2+}]_{cyt}$ following stimulation with ATP (100 μM) after incubation with $P2Y_2R$- (AR-C118925XX), $P2X_4R$- (5-BDBD), and $P2X_7R$-Antagonist (A438079). Displayed are differences between maximum and baseline $[Ca^{2+}]_{cyt.}$ (Δ: delta) as box plots, with median values ± 75% and 25% quartiles, $n = 6$ for each antagonist, * $p < 0.001$ vs. baseline conditions, # $p < 0.001$ vs ctr

different as under calcium-containing conditions. However, $P2Y_2R$ knockdown in RLE cells does not entirely diminish the calcium response to ATP. This can be explained by the coexpression of a second P2YR, presumably $P2Y_4R$, as we detected the mRNA and protein of this receptor in these cells. In A549, the $P2Y_2R$ was the only relevant active receptors responsible for the ATP-induced calcium response as the respective knockdown resulted in the complete extinction of the calcium rise upon nucleotide stimulation. Interestingly, the knockdown of $P2Y_6R$ in A459 resulted, as the knockdown of $P2X_5R$ in L2 cells, in an enhanced $[Ca^{2+}]_{cyt}$ (data not shown). However, $P2Y_6R$ mRNA knockdown was almost complete, and the UDP-induced calcium response was nearly extinguished (data not shown). We speculate that the functional loss of a P2 subtype results in a compensation mechanism that leads to increased activation of other P2 subtypes. In this regard, we found that after $P2Y_6R$ knockdown, $P2X_4R$ and/or $P2X_5R$ became increasingly active, since we detected a diminished $[Ca^{2+}]_{cyt}$ response in a calcium-free environment (data not shown), which was not detected in native A549 cells. Suh et al. have shown that intervention on a G protein-coupled receptor activity can influence other receptors, presupposing a close spatial colocalization of the involved receptors [60]. Knockdown experiments in piAECs were not successful because of the differentiation of type II AECs into type I AECs in vitro, colliding with the time frame needed for the siRNA knockdown procedure. However, besides the P2YRs, P2XRs seemed to play a role in piAECs as the application of calcium-free conditions attenuates the calcium response to ATP significantly. The functional stimulation and mRNA expression, as well as the protein analysis of piAECs, revealed $P2X_4R$ and $P2X_7R$ to be the most likely functionally active P2XR candidates on piAECs. Therefore, we conducted pharmacological inhibition of $P2Y_2R$, $P2X_4R$, and $P2X_7R$. The application of the specific antagonists of the respective receptors led to the assumption that the three mentioned receptors were to be equally involved in the increase of ATP induced $[Ca^{2+}]_{cyt}$. This result supports our assumption that subpopulations expressing different P2Rs as well as having different P2R profiles on the apical and basolateral membranes might exist as discussed for L2 cells as well.

In summary, the findings for each cell line suggest that predominant P2Rs on primarily isolated and immortalized AECs are $P2Y_2R$ and $P2Y_6R$ regarding the P2YR family and $P2X_4R$ as well as $P2X_7R$ concerning the P2XR family (Fig. 9). In all investigated AEC lines and piAECs the $P2Y_2R$ plays a dominant role in the ATP-induced rise in $[Ca^{2+}]_{cyt}$. However, other distinct P2Rs are involved in the ATP-triggered $[Ca^{2+}]_{cyt}$ increase as well, like $P2Y_6R$ (L2 and R3/1), $P2X_4R$ (L2 and piAECs), and $P2X_7R$ (piAECs).

The combination of mRNA detection, analysis of membrane receptor expression, pharmacological testing by live-cell calcium imaging and receptor siRNA knockdown provided profound insight into P2R expression and functionality in piAECs and multiple AEC lines. Although much research has been conducted in this field, the literature is often inconsistent, and the methods of P2R identification differ (chemical analysis, pharmacological testing, mRNA detection, immune staining). Often, only a selection of P2R subtypes is focused on at one time [61–64]. Because purinergic signaling is a potent but sensitive regulator of a diversity of cellular processes, including danger signals, inflammation, and the stress response, it is likely that even minor changes in the extracellular environment, such as cell culture conditions or the method of cell isolation, have an impact on P2 expression and can account for inconsistent findings in the literature. Knowledge of the respective P2 expression profile of a

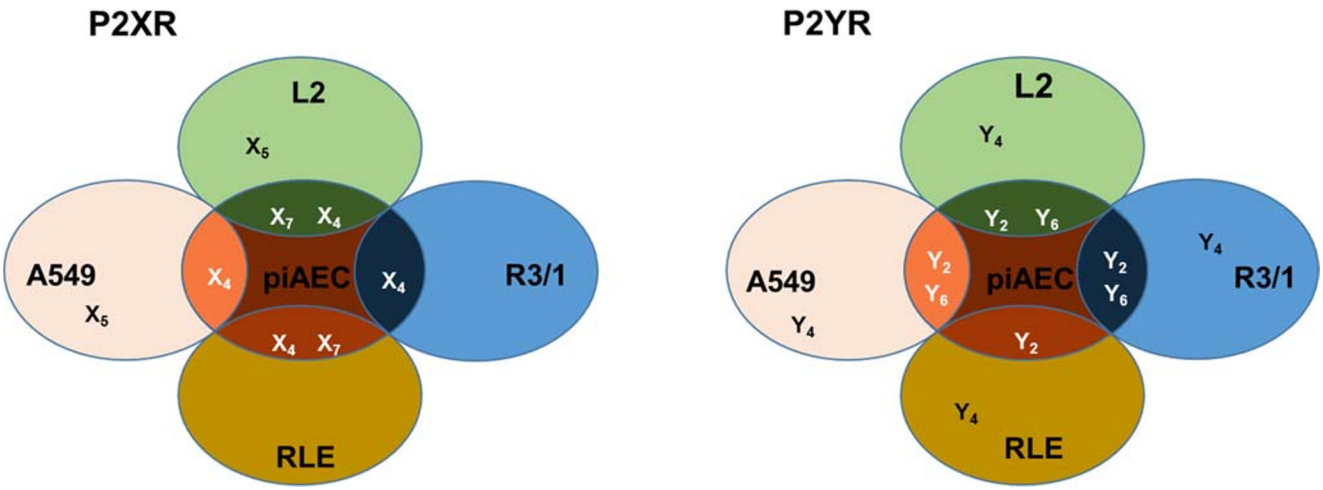

Fig. 9 Synopsis of the expression and functionality of P2XRs and P2YRs in the AEC lines investigated in comparison to primary isolated AECs

cell line is crucial when performing research on purinergic signaling pathways and in the future, even more of the many common immortalized and tumor-derived AEC lines have to be characterized concerning this matter.

Acknowledgments The authors wish to thank Kirsten Pfeiffer-Drenkhahn, Andrea Pawelczyk, Claudia Luechau, and Monika Weber for their great technical assistance. Without it, this work would not have been possible. Furthermore, the authors gratefully acknowledge the assistance of Gerhard Schoen from the Institute of Medical Biometry and Epidemiology at the University of Hamburg who guided and helped with the statistical data analysis.

Compliance with ethical standards

Conflict of interest The authors declare that they have no conflict of interests.

Ethical approval This article does not contain any studies with human participants or animals performed by any of the authors.

References

1. Guillot L, Nathan N, Tabary O, Thouvenin G, Le Rouzic P, Corvol H, Amselem S, Clement A (2013) Alveolar epithelial cells: master regulators of lung homeostasis. Int J Biochem Cell Biol 45(11): 2568–2573. https://doi.org/10.1016/j.biocel.2013.08.009
2. Parker D, Prince A (2011) Innate immunity in the respiratory epithelium. Am J Respir Cell Mol Biol 45(2):189–201. https://doi.org/10.1165/rcmb.2011-0011RT
3. Peteranderl C, Sznajder JI, Herold S, Lecuona E (2017) Inflammatory responses regulating alveolar ion transport during pulmonary infections. Front Immunol 8:446. https://doi.org/10.3389/fimmu.2017.00446
4. Lee IT, Lin CC, Lin WN, Wu WL, Hsiao LD, Yang CM (2013) Lung inflammation caused by adenosine-5′-triphosphate is mediated via Ca2+/PKCs-dependent COX-2/PGE2 induction. Int J Biochem Cell Biol 45(8):1657–1668. https://doi.org/10.1016/j.biocel.2013.05.006
5. Song S, Jacobson KN, McDermott KM, Reddy SP, Cress AE, Tang H, Dudek SM, Black SM, Garcia JG, Makino A, Yuan JX (2016) ATP promotes cell survival via regulation of cytosolic [Ca2+] and Bcl-2/Bax ratio in lung cancer cells. Am J Phys Cell Phys 310(2): C99–C114. https://doi.org/10.1152/ajpcell.00092.2015
6. Reutershan J, Vollmer I, Stark S, Wagner R, Ngamsri KC, Eltzschig HK (2009) Adenosine and inflammation: CD39 and CD73 are critical mediators in LPS-induced PMN trafficking into the lungs. FASEB J 23(2):473–482. https://doi.org/10.1096/fj.08-119701
7. Hasan D, Blankman P, Nieman GF (2017) Purinergic signalling links mechanical breath profile and alveolar mechanics with the pro-inflammatory innate immune response causing ventilation-induced lung injury. Purinergic Signal 13:363–386. https://doi.org/10.1007/s11302-017-9564-5
8. North RA (2002) Molecular physiology of P2X receptors. Physiol Rev 82(4):1013–1067. https://doi.org/10.1152/physrev.00015.2002
9. Burnstock G (2014) Purinergic signalling: from discovery to current developments. Exp Physiol 99(1):16–34. https://doi.org/10.1113/expphysiol.2013.071951
10. Coddou C, Yan Z, Obsil T, Huidobro-Toro JP, Stojilkovic SS (2011) Activation and regulation of purinergic P2X receptor channels. Pharmacol Rev 63(3):641–683. https://doi.org/10.1124/pr.110.003129
11. Burnstock G, Boeynaems JM (2014) Purinergic signalling and immune cells. Purinergic Signal 10(4):529–564. https://doi.org/10.1007/s11302-014-9427-2
12. Burnstock G, Ralevic V (2014) Purinergic signaling and blood vessels in health and disease. Pharmacol Rev 66(1):102–192. https://doi.org/10.1124/pr.113.008029
13. Tan JJ, Boudreault F, Adam D, Brochiero E, Grygorczyk R (2019) Type 2 secretory cells are primary source of ATP release in mechanically-stretched lung alveolar cells. Am J Phys Lung Cell Mol Phys. https://doi.org/10.1152/ajplung.00321.2019
14. Corriden R, Insel PA (2010) Basal release of ATP: an autocrine-paracrine mechanism for cell regulation. Sci Signal 3(104):re1. https://doi.org/10.1126/scisignal.3104re1
15. Idzko M, Ferrari D, Eltzschig HK (2014) Nucleotide signalling during inflammation. Nature 509(7500):310–317. https://doi.org/10.1038/nature13085
16. Jacobson KA, Paoletta S, Katritch V, Wu B, Gao ZG, Zhao Q, Stevens RC, Kiselev E (2015) Nucleotides acting at P2Y receptors: connecting structure and function. Mol Pharmacol 88(2):220–230. https://doi.org/10.1124/mol.114.095711
17. Berridge MJ, Bootman MD, Roderick HL (2003) Calcium signalling: dynamics, homeostasis and remodelling. Nat Rev Mol Cell Biol 4(7):517–529. https://doi.org/10.1038/nrm1155
18. Burnstock G (2007) Purine and pyrimidine receptors. Cell Mol Life Sci 64(12):1471–1483. https://doi.org/10.1007/s00018-007-6497-0
19. Vaughn BP, Robson SC, Burnstock G (2012) Pathological roles of purinergic signaling in the liver. J Hepatol 57(4):916–920. https://doi.org/10.1016/j.jhep.2012.06.008
20. Junger WG (2011) Immune cell regulation by autocrine purinergic signalling. Nat Rev Immunol 11(3):201–212. https://doi.org/10.1038/nri2938
21. Zhao H, Kilgas S, Alam A, Eguchi S, Ma D (2016) The role of extracellular adenosine triphosphate in ischemic organ injury. Crit Care Med 44(5):1000–1012. https://doi.org/10.1097/ccm.0000000000001603
22. Belete HA, Hubmayr RD, Wang S, Singh RD (2011) The role of purinergic signaling on deformation induced injury and repair responses of alveolar epithelial cells. PLoS One 6(11):e27469. https://doi.org/10.1371/journal.pone.0027469
23. Muller T, Bayer H, Myrtek D, Ferrari D, Sorichter S, Ziegenhagen MW, Zissel G, Virchow JC Jr, Luttmann W, Norgauer J, Di Virgilio F, Idzko M (2005) The P2Y14 receptor of airway epithelial cells: coupling to intracellular Ca2+ and IL-8 secretion. Am J Respir Cell Mol Biol 33(6):601–609. https://doi.org/10.1165/rcmb.2005-0181OC
24. Miraglia E, Hogberg J, Stenius U (2012) Statins exhibit anticancer effects through modifications of the pAkt signaling pathway. Int J Oncol 40(3):867–875. https://doi.org/10.3892/ijo.2011.1223
25. Thompson KE, Korbmacher JP, Hecht E, Hobi N, Wittekindt OH, Dietl P, Kranz C, Frick M (2013) Fusion-activated cation entry (FACE) via P2X(4) couples surfactant secretion and alveolar fluid transport. FASEB J 27(4):1772–1783. https://doi.org/10.1096/fj.12-220533
26. Garcia-Verdugo I, Ravasio A, de Paco EG, Synguelakis M, Ivanova N, Kanellopoulos J, Haller T (2008) Long-term exposure to LPS enhances the rate of stimulated exocytosis and surfactant secretion in alveolar type II cells and upregulates P2Y2 receptor expression. Am J Phys Lung Cell Mol Phys 295(4):L708–L717. https://doi.org/10.1152/ajplung.00536.2007
27. Dobbs LG (1990) Isolation and culture of alveolar type II cells. Am J Phys 258(4 Pt 1):L134–L147
28. Dobbs LG GR (2002) Culture of epithelial cells. Isolation and culture of alveolar type II cells, vol second edition

29. Beers MF, Moodley Y (2017) When is an alveolar type 2 cell an alveolar type 2 cell? A conundrum for lung stem cell biology and regenerative medicine. Am J Respir Cell Mol Biol 57(1):18–27. https://doi.org/10.1165/rcmb.2016-0426PS
30. Miklavc P, Ehinger K, Thompson KE, Hobi N, Shimshek DR, Frick M (2014) Surfactant secretion in LRRK2 knock-out rats: changes in lamellar body morphology and rate of exocytosis. PLoS One 9(1): e84926. https://doi.org/10.1371/journal.pone.0084926
31. Isakson BE, Lubman RL, Seedorf GJ, Boitano S (2001) Modulation of pulmonary alveolar type II cell phenotype and communication by extracellular matrix and KGF. Am J Phys Cell Phys 281(4):C1291–C1299
32. Kaestle SM, Reich CA, Yin N, Habazettl H, Weimann J, Kuebler WM (2007) Nitric oxide-dependent inhibition of alveolar fluid clearance in hydrostatic lung edema. Am J Phys Lung Cell Mol Phys 293(4):L859–L869. https://doi.org/10.1152/ajplung.00008.2007
33. Nguyen T, Erb L, Weisman GA, Marchese A, Heng HH, Garrad RC, George SR, Turner JT, O'Dowd BF (1995) Cloning, expression, and chromosomal localization of the human uridine nucleotide receptor gene. J Biol Chem 270(52):30845–30848
34. Barrett MO, Sesma JI, Ball CB, Jayasekara PS, Jacobson KA, Lazarowski ER, Harden TK (2013) A selective high-affinity antagonist of the P2Y14 receptor inhibits UDP-glucose-stimulated chemotaxis of human neutrophils. Mol Pharmacol 84(1):41–49. https://doi.org/10.1124/mol.113.085654
35. Chambers JK, Macdonald LE, Sarau HM, Ames RS, Freeman K, Foley JJ, Zhu Y, McLaughlin MM, Murdock P, McMillan L, Trill J, Swift A, Aiyar N, Taylor P, Vawter L, Naheed S, Szekeres P, Hervieu G, Scott C, Watson JM, Murphy AJ, Duzic E, Klein C, Bergsma DJ, Wilson S, Livi GP (2000) A G protein-coupled receptor for UDP-glucose. J Biol Chem 275(15):10767–10771
36. Penuela S, Gehi R, Laird DW (2013) The biochemistry and function of pannexin channels. Biochim Biophys Acta 1828(1):15–22. https://doi.org/10.1016/j.bbamem.2012.01.017
37. Rooney SA (2001) Regulation of surfactant secretion. Comp Biochem Physiol A Mol Integr Physiol 129(1):233–243
38. Furuya K, Tan JJ, Boudreault F, Sokabe M, Berthiaume Y, Grygorczyk R (2016) Real-time imaging of inflation-induced ATP release in the ex vivo rat lung. Am J Phys Lung Cell Mol Phys 311(5):L956–l969. https://doi.org/10.1152/ajplung.00425.2015
39. Seminario-Vidal L, Kreda S, Jones L, O'Neal W, Trejo J, Boucher RC, Lazarowski ER (2009) Thrombin promotes release of ATP from lung epithelial cells through coordinated activation of rho- and Ca2+−dependent signaling pathways. J Biol Chem 284(31): 20638–20648. https://doi.org/10.1074/jbc.M109.004762
40. Tatur S, Kreda S, Lazarowski E, Grygorczyk R (2008) Calcium-dependent release of adenosine and uridine nucleotides from A549 cells. Purinergic Signal 4(2):139–146. https://doi.org/10.1007/s11302-007-9059-x
41. Burnstock G, Evans LC, Bailey MA (2014) Purinergic signalling in the kidney in health and disease. Purinergic Signal 10(1):71–101. https://doi.org/10.1007/s11302-013-9400-5
42. Lowenstern A, Storey RF, Neely M, Sun JL, Angiolillo DJ, Cannon CP, Himmelmann A, Huber K, James SK, Katus HA, Morais J, Siegbahn A, Steg PG, Wallentin L, Becker RC (2017) Platelet-related biomarkers and their response to inhibition with aspirin and p2y12-receptor antagonists in patients with acute coronary syndrome. J Thromb Thrombolysis 44(2):145–153. https://doi.org/10.1007/s11239-017-1516-y
43. Bagai A, Peterson ED, McCoy LA, Effron MB, Zettler ME, Stone GW, Henry TD, Cohen DJ, Schulte PJ, Anstrom KJ, Wang TY (2017) Association of measured platelet reactivity with changes in P2Y12 receptor inhibitor therapy and outcomes after myocardial infarction: insights into routine clinical practice from the TReatment with ADP receptor iNhibitorS: Longitudinal Assessment of Treatment Patterns and Events after Acute Coronary Syndrome (TRANSLATE-ACS) study. Am Heart J 187:19–28. https://doi.org/10.1016/j.ahj.2017.02.003
44. Di Virgilio F, Dal Ben D, Sarti AC, Giuliani AL, Falzoni S (2017) The P2X7 receptor in infection and inflammation. Immunity 47(1): 15–31. https://doi.org/10.1016/j.immuni.2017.06.020
45. von Kugelgen I, Hoffmann K (2016) Pharmacology and structure of P2Y receptors. Neuropharmacology 104:50–61. https://doi.org/10.1016/j.neuropharm.2015.10.030
46. Takai E, Tsukimoto M, Harada H, Sawada K, Moriyama Y, Kojima S (2012) Autocrine regulation of TGF-beta1-induced cell migration by exocytosis of ATP and activation of P2 receptors in human lung cancer cells. J Cell Sci 125(Pt 21):5051–5060. https://doi.org/10.1242/jcs.104976
47. Dreisig K, Kornum BR (2016) A critical look at the function of the P2Y11 receptor. Purinergic Signal 12(3):427–437. https://doi.org/10.1007/s11302-016-9514-7
48. Miklavc P, Thompson KE, Frick M (2013) A new role for P2X4 receptors as modulators of lung surfactant secretion. Front Cell Neurosci 7:171. https://doi.org/10.3389/fncel.2013.00171
49. Gicquel T, Le Dare B, Boichot E, Lagente V (2017) Purinergic receptors: new targets for the treatment of gout and fibrosis. Fundam Clin Pharmacol 31(2):136–146. https://doi.org/10.1111/fcp.12256
50. Burnstock G (2016) P2X ion channel receptors and inflammation. Purinergic Signal 12(1):59–67. https://doi.org/10.1007/s11302-015-9493-0
51. Chen Z, Jin N, Narasaraju T, Chen J, McFarland LR, Scott M, Liu L (2004) Identification of two novel markers for alveolar epithelial type I and II cells. Biochem Biophys Res Commun 319(3):774–780. https://doi.org/10.1016/j.bbrc.2004.05.048
52. Azimi I, Beilby H, Davis FM, Marcial DL, Kenny PA, Thompson EW, Roberts-Thomson SJ, Monteith GR (2016) Altered purinergic receptor-Ca(2)(+) signaling associated with hypoxia-induced epithelial-mesenchymal transition in breast cancer cells. Mol Oncol 10(1):166–178. https://doi.org/10.1016/j.molonc.2015.09.006
53. Shabbir M, Burnstock G (2009) Purinergic receptor-mediated effects of adenosine 5′-triphosphate in urological malignant diseases. Int J Urol 16(2):143–150. https://doi.org/10.1111/j.1442-2042.2008.02207.x
54. Le KT, Paquet M, Nouel D, Babinski K, Seguela P (1997) Primary structure and expression of a naturally truncated human P2X ATP receptor subunit from brain and immune system. FEBS Lett 418(1–2):195–199
55. Dietl P, Liss B, Felder E, Miklavc P, Wirtz H (2010) Lamellar body exocytosis by cell stretch or purinergic stimulation: possible physiological roles, messengers and mechanisms. Cell Physiol Biochem 25(1):1–12. https://doi.org/10.1159/000272046
56. Murthy KS, Makhlouf GM (1998) Coexpression of ligand-gated P2X and G protein-coupled P2Y receptors in smooth muscle. Preferential activation of P2Y receptors coupled to phospholipase C (PLC)-beta1 via Galphaq/11 and to PLC-beta3 via Gbetagammai3. J Biol Chem 273(8):4695–4704
57. Hervas C, Perez-Sen R, Miras-Portugal MT (2003) Coexpression of functional P2X and P2Y nucleotide receptors in single cerebellar granule cells. J Neurosci Res 73(3):384–399. https://doi.org/10.1002/jnr.10676
58. Zhu H, Yu Y, Zheng L, Wang L, Li C, Yu J, Wei J, Wang C, Zhang J, Xu S, Wei X, Cui W, Wang Q, Chen X (2015) Chronic inflammatory pain upregulates expression of P2Y2 receptor in small-diameter sensory neurons. Metab Brain Dis 30(6):1349–1358. https://doi.org/10.1007/s11011-015-9695-8
59. Volonte C, Amadio S, D'Ambrosi N, Colpi M, Burnstock G (2006) P2 receptor web: complexity and fine-tuning. Pharmacol Ther 112(1):264–280. https://doi.org/10.1016/j.pharmthera.2005.04.012

60. Suh BC, Kim JS, Namgung U, Han S, Kim KT (2001) Selective inhibition of beta(2)-adrenergic receptor-mediated cAMP generation by activation of the P2Y(2) receptor in mouse pineal gland tumor cells. J Neurochem 77(6):1475–1485
61. Laubinger W, Reiser G (1998) Differential characterization of binding sites for adenine and uridine nucleotides in membranes from rat lung as possible tools for studying P2 receptors in lung. Biochem Pharmacol 55(5):687–695
62. Clunes MT, Collett A, Baines DL, Bovell DL, Murphie H, Inglis SK, McAlroy HL, Olver RE, Wilson SM (1998) Culture substrate-specific expression of P2Y2 receptors in distal lung epithelial cells isolated from foetal rats. Br J Pharmacol 124(5):845–847. https://doi.org/10.1038/sj.bjp.0701942
63. Factor P, Mutlu GM, Chen L, Mohameed J, Akhmedov AT, Meng FJ, Jilling T, Lewis ER, Johnson MD, Xu A, Kass D, Martino JM, Bellmeyer A, Albazi JS, Emala C, Lee HT, Dobbs LG, Matalon S (2007) Adenosine regulation of alveolar fluid clearance. Proc Natl Acad Sci U S A 104(10):4083–4088. https://doi.org/10.1073/pnas.0601117104
64. Burnstock G, Brouns I, Adriaensen D, Timmermans JP (2012) Purinergic signaling in the airways. Pharmacol Rev 64(4):834–868. https://doi.org/10.1124/pr.111.005389